

Fig. 3. Electron micrograph of undecomposed  $\gamma$ -FeOOH showing (120) lattice planes of spacing 3.3 Å, Hitachi HU-12A. Magnification 5 000 000

sed platelets, the undecomposed regions, exhibit the usual extinction contours (Bragg fringes) which show that this part of the lattice is scattering coherently\*. In a few cases it was possible to make directly visible the (120) lattice planes of  $\gamma$ -FeOOH in undecomposed crystals (fig. 3).

#### 4 Discussion and conclusions

The kinetical data (fig. 2) fit equally well into quite different functions as shown in the representation of SHARP *et al.*<sup>8</sup> (Fig. 5). An unambiguous answer from these results alone, hence, is impossible.

The additional evidence from electron micrographs, X-ray diffraction, electron diffraction and BET surface measurements, however, suggests the following mechanism.

In order to form the  $\gamma$ -Fe<sub>2</sub>O<sub>3</sub> lattice, the corrugated layers of edge and corner sharing (FeO<sub>6</sub>) octahedra of  $\gamma$ -FeOOH must collapse in the manner shown schematically in fig. 6. By the introduction of more edge and corner sharing, O<sup>2-</sup> ions in the form of water are set free. The considerable lattice strain visualized in fig. 6 accompanied by additional shear in the two other directions of the lattice leads to the total disruption of the dehydrated region of  $\gamma$ -FeOOH. The front of such a region being under strain is a suitable nucleus for further reaction; the process thus continues along the needle axis *c*, starting usually from cracks or other defects at the edge of the crystal. The strings of 70 Å large  $\gamma$ -Fe<sub>2</sub>O<sub>3</sub> crystallites produce the mentioned contrast phenomenon since their neighbourhood has to support

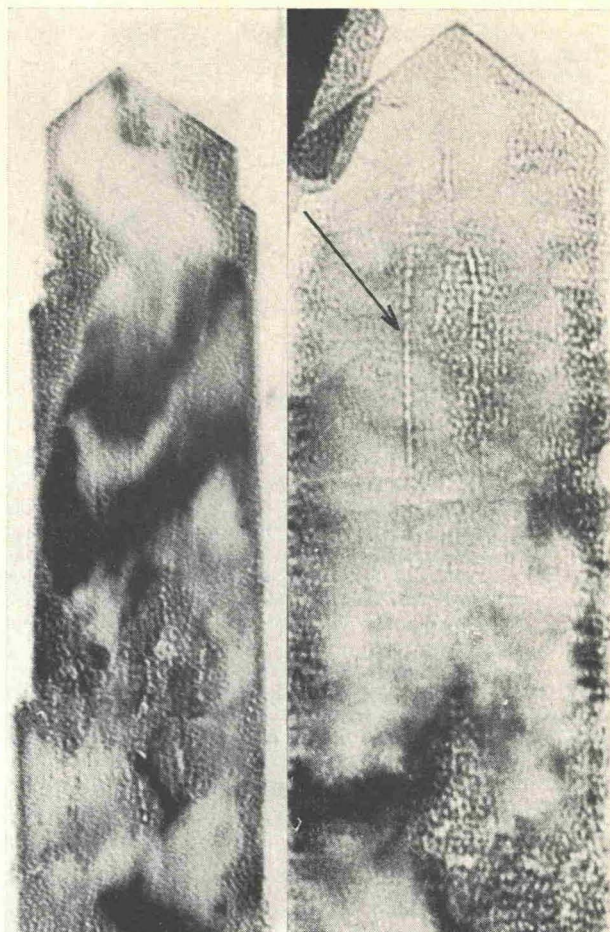


Fig. 4. Electron micrographs of partly decomposed  $\gamma$ -FeOOH crystals. Uniform grey regions with black extinction contours (Bragg fringes) are unaltered; the granular structure of other regions indicates complete dehydration. Instead of a sharp phase boundary, pearl-like strings intrude from decomposed regions into regions of unaltered  $\gamma$ -FeOOH. The visible crystallite size is consistent with 70 Å found from X-ray reflection profiles. BET measurements of the specific surface show that these features are not pores; hence they are crystallites of  $\gamma$ -Fe<sub>2</sub>O<sub>3</sub> producing a considerable strain on the surrounding matrix, thus giving the contrast phenomenon. Arrow indicates strings of  $\gamma$ -Fe<sub>2</sub>O<sub>3</sub>. Magnification 200 000

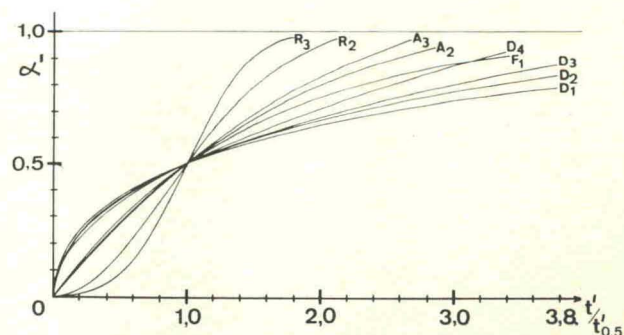


Fig. 5. Calculated rate curves representing various models of reaction mechanisms, after SHARP *et al.*<sup>8</sup> Reduced time scale and ordinate as fig. 2. F 1 = First order law (Random nucleation), D 1 to 4 = diffusion controlled mechanisms, A = Avrami equations, R = boundary controlled mechanism. For full explanation see reference<sup>8</sup>

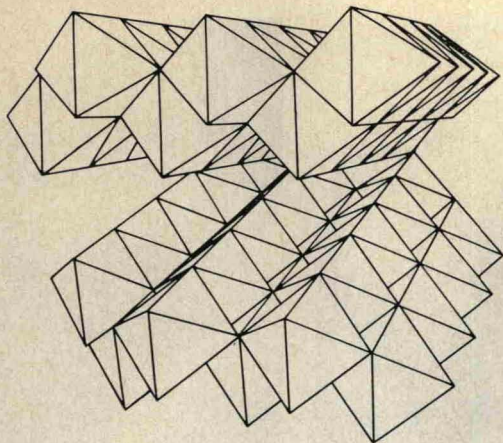


Fig. 6. Schematic three-dimensional representation of interface between undecomposed  $\gamma$ -FeOOH and final  $\gamma$ -Fe<sub>2</sub>O<sub>3</sub>, producing the considerable strain in the  $\gamma$ -FeOOH crystal and the contrast effect in the electron micrograph. The front of the picture represents the boehmite type lattice of  $\gamma$ -FeOOH (hydrogen bonds holding together the corrugated layers are omitted). Towards the background these layers approach each other until they collapse (in the back end of the figure).

From there the octahedra would extend further backwards forming essentially a cubic dense packing, i. e. the  $\gamma$ -Fe<sub>2</sub>O<sub>3</sub> lattice. This representation showing the transition between the two lattices makes evident the total disruption of the initial crystal into numberless microcrystallites consisting of only about 5 to 10 unit cells. It also makes evident that in these microcrystals ordering to the perfect  $\gamma$ -Fe<sub>2</sub>O<sub>3</sub> structure is not possible.

considerable shear and other strain. The contrast is best visible in the early stage of the dehydration, when it shows particularly well against the Bragg fringes of the surrounding undecomposed matrix.

The final product has still a crystallite size of 70 Å. The residual water is therefore chemisorbed and cannot take off even *in vacuo*, hence the sluggish end part of the reaction. This might lead to the erroneous conclusion that  $\gamma$ -Fe<sub>2</sub>O<sub>3</sub> is stable only in the presence of protons. FEITKNECHT<sup>1,2</sup> and GALLAGHER<sup>3</sup> have, however, shown that this view is incorrect.

The small crystallite size and the low temperature seem to suppress the rearrangement of the lattice disorder, as opposed to the ordering observed in  $\gamma$ -Fe<sub>2</sub>O<sub>3</sub> cubes of about 30 times larger size in O<sub>2</sub> atmosphere.

A full account on this subject will be submitted to *Thermochemica Acta*.

We thank Professor W. FEITKNECHT and Dr. K. J. GALLAGHER for helpful discussions, Dr. H.-G. WIEDEMANN (Mettler Ltd.) for permission to use apparatus and for other support, Mr. T. KAMINO for help to obtain lattice resolution, Miss ETTINGER for photographic work, and the Swiss National Fund for financial support.

RUDOLF GIOVANOLI und RUDOLF BRÜTSCH

Laboratory of Electron Microscopy  
Institute of Inorganic Chemistry  
University of Berne  
Freiestrasse 3  
P.O.B. 140, CH-3000 Berne 9 (Switzerland)

\* Bragg fringes are bands in which the Bragg condition for diffraction is fulfilled and where coherently scattered parts of the electron beam are caught at the contrast aperture. Such "extinction contours" are therefore dark<sup>7</sup>.

<sup>7</sup> L. REIMER, *Elektronenmikroskopische Untersuchungs- und Präparationsmethoden*, 2nd Edition, Springer, Berlin 1967, p. 191 ff.

<sup>8</sup> J. H. SHARP, G. W. BRINDLEY and B. N. NARAHARI ACHAR, *J. Amer. Ceram. Soc.* 49 (1966) 379.